Available online at www.sciencedirect.com
SCIENCE DIRECT®
ELSEVIER
Talanta 69 (2006) 946–951
Talanta
www.elsevier.com/locate/talanta

Novel low humidity sensor made of TiO_2 nanowires/poly(2-acrylamido-2-methylpropane sulfonate) composite material film combined with quartz crystal microbalance

Pi-Guey Su [a,*], Yi-Lu Sun [b], Chu-Chieh Lin [b,**]

[a] Department of Chemistry, Chinese Culture University, Taipei 111, Taiwan
[b] Department of Chemistry, National Chung-Hsing University, Taichung 402, Taiwan

Received 29 August 2005; received in revised form 22 November 2005; accepted 22 November 2005

Abstract

A novel ceramic nanowires of TiO_2 and poly(2-acrylamido-2-methylpropane sulfonate) (TiO_2 NWs/PAMPS) composite material films coated on quartz crystal microbalance (QCM) was prepared as a low humidity sensor. The 50 wt.% of TiO_2 NWs/PAMPS composite material films showed excellent sensitivity ($2.63 - \Delta Hz/\Delta ppm_v$) at 31.5 ppm_v), linearity ($R^2 = 0.9959$) and acceptable response time (64 s at 34.6 ppm_v). The low humidity sensing mechanism was discussed in terms of surface texture and nanostructured morphology of the composite materials. Moreover, the adsorption dynamic analysis, molecular mechanics calculation (association constant), was used to elucidate the effect of adding 50 wt.% TiO_2 NWs into PAMPS in the increased sensitivity of low humidity sensing.

Keywords: Low humidity sensor; Quartz crystal microbalance; Composite material; TiO_2 nanowires; PAMPS; Adsorption dynamic analysis

1. Introduction

Humidity measurements are very important concerns in environmental fields, such as medical or domestic applications for human comfort, industrial uses, agriculture, automobiles, textiles, etc. [1]. There are many kinds of ceramics, organic polymers and composite materials have been studied for the development of humidity sensors. Inorganic semiconducting oxides like aluminium oxide (Al_2O_3), tin oxide (SnO_2), iron oxide (Fe_2O_3), zinc oxide (ZnO) and titanium oxide (TiO_2) have been studied as humidity sensors [2–5]. The polymer electrolytes are one of interesting materials because they have a better humidity-sensitive characteristic, such as long-term stability, reliability, ease of processing and the low fabrication cost, than the ceramic materials. For example, poly(2-acrylamido-2-methylpropane sulfonate) (PAMPS) polymer electrolyte with acidic groups or their salts, such as $-SO^{3-}H^+$ or $-SO^{3-}M^+$, where M is an alkali metal has been used for humidity sensors material [6–10]. Some composite materials of inorganic/polymer have been reported as humidity sensors, such as SiO_2/Nafion [11], TEOS/PAMPS [10], $BaTiO_3$/RMX [12,13] and $BaTiO_3$/polystrene sulfonic sodium [14].

Different sensing techniques, impedance, capacity [15], optic [16], field effect transistors (FET) [17,18], surface acoustic wave (SAW) [19] and quartz crystal microbalance (QCM) [20–24] have been explored to detect the humidity. Among above various sensing technologies for humidity detection, the QCM is a very stable device, capable of measuring an extremely small mass change [25]. The apparent mass was modified and so was the resonant frequency, a hygroscopic material has been laid on the quartz to increase the sensitivity by adsorption of water and the mass was sharply modified by humidity of ambient air. The quantitative analysis of the mass change causes by the original Sauerbrey equation as follows [26]:

$$\Delta f = \left(-2.3 \times 10^6 \frac{f_o^2}{A}\right) \Delta m \qquad (1)$$

---

* Corresponding author. Tel.: +886 2 28610511x375; fax: +886 2 28614212.
** Co-corresponding author. Tel.: +886 4 22840411x718; fax: +886 4 22862547.
E-mail addresses: spg@faculty.pccu.edu.tw (P.-G. Su), cchlin@mail.nchu.edu.tw (C.-C. Lin).

0039-9140/$ – see front matter © 2005 Elsevier B.V. All rights reserved.
doi:10.1016/j.talanta.2005.11.039

where Δf (MHz) is the change in frequency, f_0 the foundation resonance frequency of the crystal, A (cm^2) the surface area of the electrode and Δm (g) is the change in mass on the surface of the crystal.

The hygroscopic materials were prepared as films coated on the electrode of QCM in order to detect various vapor and humidity, such as modified nitrated polystyrene [20], QCM associated with Peltier device [21] and Nafion–Ag [22]. The nanomaterials were also used as sensing films, such as nanosized zeolite film [23] and single-walled carbon nanotube/Nafion composite material [24], the sensitivities were enhanced and that were also very interesting subjects for further study. However, there was no nanocomposite material made of nanostructured ceramic materials and polymer electrolytes used for low humidity sensor.

The nanostructured ceramic materials had high humidity sensitivity due to the capillary nanopores and special surface characteristics [4,5] so that in this study, a novel nanocomposite humidity sensing film was prepared by TiO_2 nanowires (TiO_2 NWs) and PAMPS as low humidity sensor. The humidity sensing characteristics of TiO_2 NWs/PAMPS films were investigated in the volume ratio of moist air range of 31.5–2170 ppm$_v$. Compared with the adsorption dynamics of water vapor molecules onto the PAMPS and 50 wt.% TiO_2 NWs/PAMPS films coated on QCM to elucidate the increased in humidity sensing sensitivity of PAMPS with addition of TiO_2 NWs.

2. Experimental

2.1. Material preparation

2.1.1. TiO_2 nanowires

TiO_2 NWs were prepared using hydrothermal method similar to that described by Li and co-workers [27]. Two grams of Anatase TiO_2 powders (Sigma–Aldrich Co. Inc., USA) was placed into a Teflon-lined autoclave of 125 ml capacity. Then, the autoclave was filled with 80 ml of 10 M NaOH aqueous solution, sealed into a stainless steel tank and maintained at 200 °C for 24 h without shaking or stirring. After the autoclave was cooled to room temperature naturally, the obtained sample was washed with dilute HCl aqueous solution, deionized (D.I.) water and ethanol sequentially several times. The fibrous white product was obtained after drying the sample at 70 °C for 6 h. Fig. 1 shows SEM image of the prepared TiO_2 NWs. It indicates the NWs are quite clean and loosened, and easy being dispersed by sonication treatment could be proposed.

2.1.2. Poly(2-acrylamido-2-methylpropane sulfonate)

The PAMPS was prepared according to the method previously described [10] by dissolving 4 g AMPS monomer (Merck) in 10 ml D.I. water, then added 0.8 ml of 0.625 wt.% sodium persulfate (Merck) in the solution. The mixture solution was refluxed at 100 °C for 15 min with high speed stirring, then poured it out and cooled to room temperature naturally. Finally, the PAMPS was diluted by 10 times with addition D.I. water.

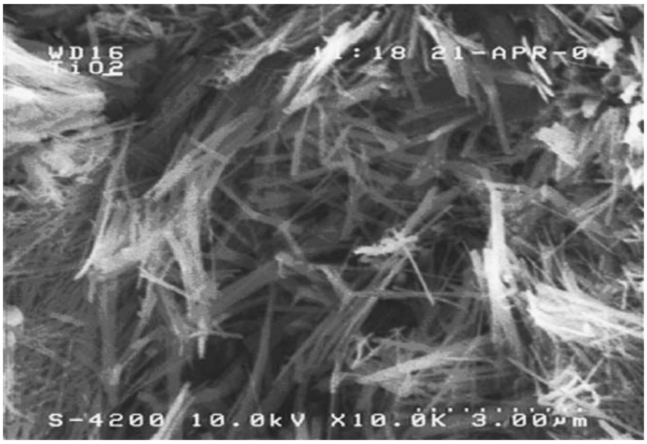

Fig. 1. FE-SEM micrograph of TiO_2 NWs.

2.1.3. TiO_2 NWs/PAMPS composite materials

The composite materials were prepared by adding of TiO_2 NWs into the diluted PAMPS solution by different weight percentages as 0, 1, 10 and 50 wt.% of TiO_2 NWs composition in the mixtures. Then, dispersed the TiO_2 NWs of the prepared samples by sonication treatment for 10 min, the white solutions were obtained.

2.2. Electrode of QCM fabrication

AT-cut quartz crystals with a fundamental resonance frequency of 9 MHz were obtained from ANT Technologies Corp. The gold electrode of the QCM was rinsed with D.I. water and then cleaned ultrasonically in acetone. After drying, both sides of the QCM electrode were coated with the mixture solution by spin coating at the speed of 1000 rpm for 60 s. A sensing film was formed by oven drying at 100 °C for 1 h in air, the thickness of the films were about 2.5–3 μm by SEM observation. All experiments were performed at room temperature about 23.0 ± 1.5 °C.

2.3. Instruments and analysis

A divided humidity generator was used as the principal facility for producing the testing gases. The required water vapor concentration was produced by adjusting the proportion of dry and humid air, generated by the divided flow humidity generator. The lowest testing point is limited by the dryness of the gas. A low humidity hygrometer (HYGROCLIP IC-3, Rotronic Inc.) and a QCM sensor was connected to an outlet of the divided flow humidity generator, and the low humidity hygrometer was used as the reference standard for the calibration of the QCM sensor. The volume ratio of the moist air would be adjusted according to the reading of the low humidity hygrometer calibrating to the Center for Measurement Standards/National Measurement Laboratory (CMS/NML) humidity laboratory. The volume ratio of the moist air was calculated by the following equation:

$$\mathrm{ppm_v} = \frac{V_v}{V} \times 10^6 \qquad (2)$$

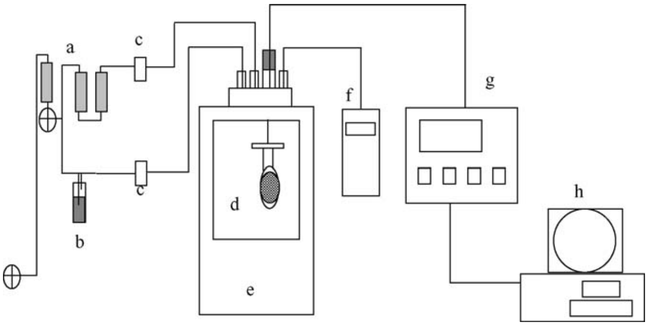

Fig. 2. Schematic diagram of experimental setup for the QCM sensor measurement and low humidity atmosphere controller. (a) Molecular sieve and desiccating agent, (b) water, (c) mass flow controller, (d) detecting chamber and QCM, (e) thermostat, (f) low humidity hygrometer, (g) oscillator and frequency counter and (h) PC.

$$\mathrm{ppm_v} = \frac{e}{P - e} \times 10^6\,(\text{ideal gas}) \qquad (3)$$

where V_v is the volume of water vapor, V the total volume, e the partial pressure of water vapor and P is the total pressure. The initial volume ratio of the moist air was 14.7 $\mathrm{ppm_v}$ for all experiments. The analysis system is illustrated in Fig. 2.

3. Results and discussion

3.1. Microstructure characteristics of TiO_2 NWs/PAMPS composite material films

The SEM images of the TiO_2 NWs/PAMPS composite material films are shown in Fig. 3. Fig. 3a, composite material film with addition of 1 wt.% of TiO_2 NWs, the TiO_2 NWs were embedded in the PAMPS films. As shown in Fig. 3b and c, there were more pulling-up TiO_2 NWs on the surface of composite material film with 50 wt.% TiO_2 NWs than that of sample with 10 wt.% TiO_2 NWs. Obviously aggregation of TiO_2 NWs was also observed in Fig. 3b and c. All these factors leaded to the difference of low humidity sensing mechanical properties.

3.2. Low humidity sensing properties of TiO_2 NWs/PAMPS composite material films

The frequency shifts and sensitivity of TiO_2 NWs/PAMPS composite material films and PAMPS films as a function of time for different volume ratio of the moist air, the range from 31.5 to 2170 $\mathrm{ppm_v}$, are plotted in Fig. 4 and is listed in Table 1. As shown in Table 1, when volume ratio of moist air was 31.5 $\mathrm{ppm_v}$, the sensitivity of 1, 10 and 50 wt.% TiO_2 NWs doped PAMPS composite material films and PAMPS films were 1.05, 1.14, 2.63 and 1.24, respectively. For TiO_2 NWs/PAMPS composite material films, the sensitivity was increased with increasing the addition amount of TiO_2 NWs. Moreover, it is definitely demonstrated that the sensitivity of 50 wt.% TiO_2 NWs doped PAMPS composite material films was higher than that of the other samples and PAMPS films, especially at humidity lower than 515 $\mathrm{ppm_v}$. However, compared with PAMPS films, the sensitivity of 1 and 10 wt.% TiO_2 NWs doped PAMPS composite material films were slightly decreased. The results of calibration curve of TiO_2 NWs/PAMPS composite material films and PAMPS films are plotted in Fig. 5 and the slope and linear correlation coefficient were calculated as shown in Table 2. For TiO_2 NWs/PAMPS composite material films, the linear sensing characteristics at the ranges of 31.5–515 and 515–2170 $\mathrm{ppm_v}$ were shown different

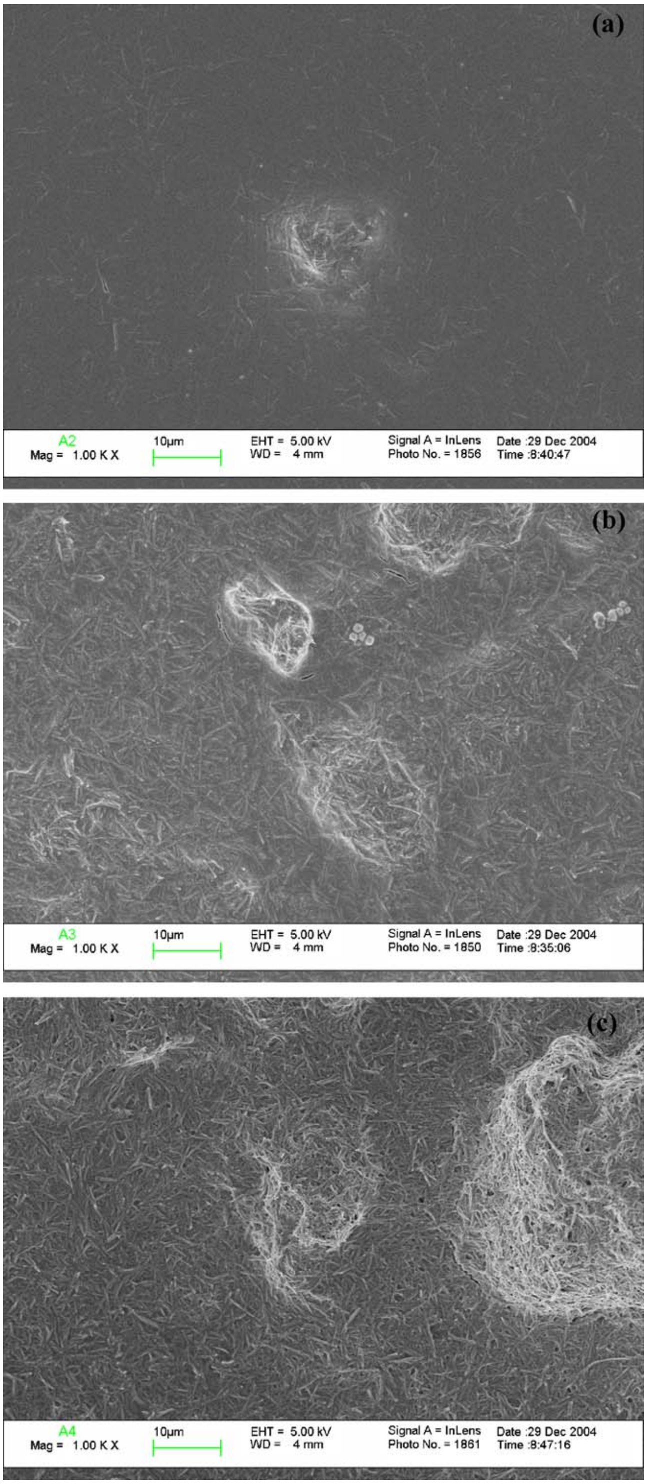

Fig. 3. FE-SEM micrographs of: (a) 1 wt.%, (b) 10 wt.% and (c) 50 wt.% TiO_2 NWs/PAMPS composite material films.

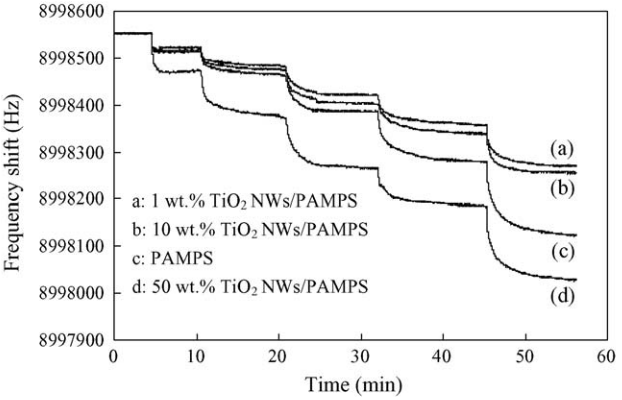

Fig. 4. (a–d) Frequency shifts (Hz) as a function of time (s) for different volume ratio of the moist air on PAMPS and various doped amount TiO_2 NWs/PAMPS composite material films.

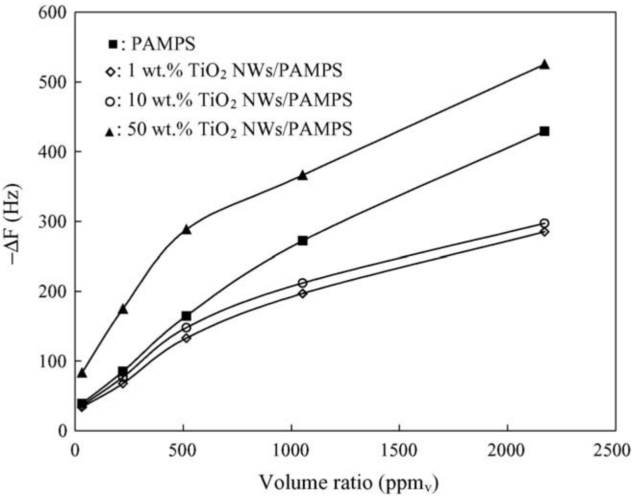

Fig. 5. Frequency changed ($-\Delta$Hz) as a function of volume ratio (ppm_v) for PAMPS and various doped amount TiO_2 NWs/PAMPS composite material films.

Table 2
The linear sensing characteristics of various doped amount of TiO_2 NWs/PAMPS composite material films and PAMPS films at different volume ratio of moist air

	Sensing characteristics			
	14.7–515 ppm_v		515–2170 ppm_v	
	Slope	Linearity[a]	Slope	Linearity[a]
PAMPS	0.2616	0.9990	0.1566	0.9918
1 wt.% TiO_2 NWs	0.2062	0.9969	0.0899	0.9882
10 wt.% TiO_2 NWs	0.2325	0.9991	0.0879	0.9860
50 wt.% TiO_2 NWs	0.4206	0.9959	0.1431	0.9998

[a] Correlation coefficient.

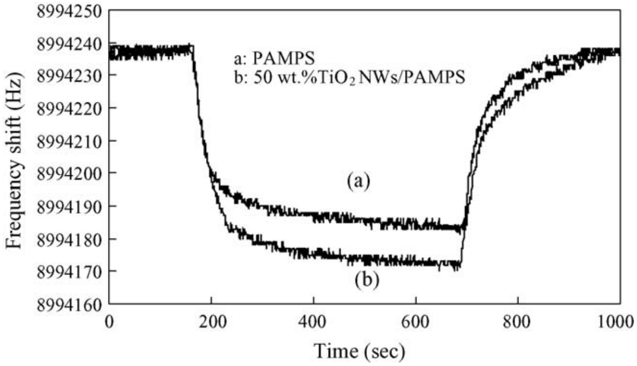

Fig. 6. Reversibility of adsorption of water vapors (34.6 ppm_v) on PAMPS films (a) and 50 wt.% TiO_2 NWs/PAMPS composite material films (b).

performance. The steep decreased in slope was observed at the volume ratio of moist air of 515–2170 ppm_v. This behavior was different from PAMPS films which showed slightly deviation in slope between the 31.5–515 and 515–2170 ppm_v. Thus, suggesting that addition of TiO_2 NWs played an important role in the low humidity sensing property. The humidity sensing of ceramic and porous materials was known to mainly occur as a surface mechanism [28]. The sensitivity of 50 wt.%TiO_2 NWs/PAMPS composite material films increased, compared to PAMPS films, was also related to the adsorption of water molecules on the surface of the composite material films. The more pulling-up tips and defects of the TiO_2 NWs on the surface of the sample with 50 wt.% TiO_2 NWs (as shown in Fig. 3c), provided more active sites, presented a high local charge density and a strong electrostatic field which promoted water dissociation on TiO_2 NWs [5,29]. But, at higher volume ratio of moist air (515–2170 ppm_v), suggested the absence of active sites for reaction to occur and, hence, the steep decreased in slope was observed. Moreover, a continuous increased in sensitivity with increasing in volume ratio of moist air was observed. This could be probably due to the PAMPS which also reacted with water molecules.

The response time (RT_{90}) and recovery time of the 50 wt.% TiO_2 NWs doped PAMPS composite material films were 64 and 184 s, respectively, at the testing point of 34.6 ppm_v (as shown in Fig. 6).

Table 1
The sensitivity of the TiO_2 NWs/PAMPS composite material films coated on QCM for different volume ratios of moist air

Volume ratio (ppm_v)	Δppm_v[a]	Sensitivity[b]			
		PAMPS	1 wt.% TiO_2 NWs	10 wt.% TiO_2 NWs	50 wt.% TiO_2 NWs
31.5	16.8	1.24	1.08	1.14	2.63
221.3	206.6	0.38	0.31	0.35	0.79
515	500.3	0.32	0.26	0.29	0.56
1052.2	1037.5	0.26	0.19	0.20	0.35
2170	2155.3	0.20	0.13	0.14	0.24

[a] The Δppm_v was defined as that the each volume ratio subtract the initial volume ratio of moisture air (14.7 ppm_v).

[b] The sensitivity of the various sensing film was defined as $-\Delta Hz/\Delta ppm_v$ [20].

Table 3
Kinetic parameters for binding and dissociation of water vapor molecules onto PAMPS films and 50 wt.% TiO_2 NWs/PAMPS composite material films

Films	Binding rate constant, k_1 (M^{-1} s^{-1})	Dissociation rate constant, k_{-1} (10^{-2} s^{-1})	Association constant, K (10^2 M^{-1})
PAMPS	80.23	0.11	744.92
50 wt.% TiO_2 NWs/PAMPS	51.00	0.07	756.60

3.3. Adsorption properties of PAMPS films and 50 wt.% TiO_2 NWs/PAMPS composite material films

In order to elucidate that the sample with 50 wt.% TiO_2 NWs increased in sensitivity, compared with PAMPS film, the adsorption dynamics of water vapor molecules onto the PAMPS and 50 wt.% TiO_2 NWs doped PAMPS composite material films coated on QCM were investigated. The results of the adsorption/desorption of water vapors (34.6 ppm_v) onto the PAMPS and 50 wt.% TiO_2 NWs/PAMPS coated on QCM are shown in Fig. 6. It was clear that the frequency shifts of the 50 wt.% TiO_2 NWs/PAMPS composite material films had the higher frequency shifts. It also appeared that desorption of water molecule from 50 wt.% TiO_2 NWs/PAMPS composite material films was relatively slower than PAMPS films. It was also observed that the process of adsorption and desorption of water on PAMPS films and 50 wt.% TiO_2 NWs/PAMPS composite material films was reversible. The results implied that 50 wt.% TiO_2 NWs doped PAMPS composite material films had larger affinity to water vapor molecules than PAMPS films.

Comparing the adsorption behaviors of water vapor molecules onto PAMPS films and 50 wt.% TiO_2 NWs/PAMPS composite material films and explanation increasing the sensitivity of humidity sensing of PAMPS films doped with TiO_2 NWs, the following reaction was adopted as the following described [22,30]:

$$\text{Sensing films} + \text{water vapor molecules} \overset{k_1}{\underset{k_{-1}}{\Leftrightarrow}} \text{sensing films–water vapor molecules} \tag{4}$$

where k_1 and k_{-1} are referred to binding rate constant and dissociation rate constant, respectively. The formed amount of water vapor molecules, Δm_t, on the sensing films at time t, is then given by the following equations under Langmuir isotherm adsorption conditions [22,30]:

$$\Delta m_t = \Delta m_\infty \left[1 - \exp\left(\frac{-t}{\tau}\right)\right] \tag{5}$$

$$\frac{-t}{\tau} = \ln\left[\frac{\Delta m_\infty - \Delta m_t}{\Delta m_\infty}\right] \tag{6}$$

$$\tau^{-1} = k_1[\text{water vapor molecules}] + k_{-1} \tag{7}$$

where Δm_∞ is the maximal adsorbed amount of water vapor molecules on sensing films at $t \to \infty$ and τ is the relaxation time. Fig. 7 shows the linear correlation between the reciprocal of the relaxation time (τ^{-1}) of adsorption and the water vapor molecules concentrations to the sensing films (PAMPS and 50 wt.% TiO_2 NWs/PAMPS). Using Fig. 7 and Eq. (7), the binding rate constant k_1, dissociation rate constant k_{-1} and association constant K ($K = \frac{k_1}{k_{-1}}$) for water vapor molecules onto the sensing films (PAMPS and 50 wt.% TiO_2 NWs/PAMPS) were calculated and are listed in Table 3. The PAMPS–water vapor molecules showed a larger k_{-1} value. This coincides with the result that water vapor molecule was easier to dissociate from PAMPS films than 50 wt.% TiO_2 NWs/PAMPS composite material films. The association constant K of water vapor molecules onto the 50 wt.% TiO_2 NWs/PAMPS sensing films were larger than PAMPS films, indicates that 50 wt.% TiO_2 NWs/PAMPS composite material films to water vapor molecules were more sensitive than PAMPS films (as shown in Tables 1 and 2).

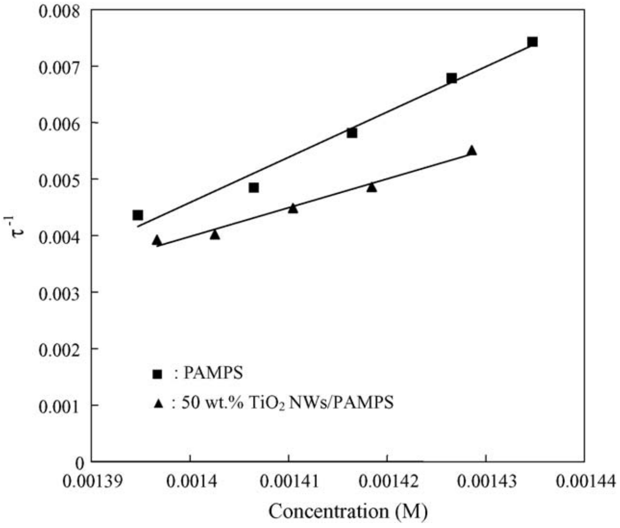

Fig. 7. Linear plot of the reciprocal of relaxation time (τ^{-1}) against vapor concentration (M) for PAMPS and 50 wt.% TiO_2 NWs/PAMPS composite material films.

4. Conclusion

A novel nanocomposite material of humidity sensing film made of 50 wt.% TiO_2 NWs and PAMPS coated on quartz crystal microbalance showed high sensitivity (especially at low humidity), good linearity and good reversibility. The possible mechanism for the 50 wt.% TiO_2 NWs/PAMPS composite material films increased sensitivity has also been suggested. The 50 wt.% TiO_2 NWs/PAMPS composite material films combines with QCM can be considered as a reliable technique for trace humidity measurement.

Based on Langmuir isotherm adsorption assumption showed larger dissociation rate constant k_{-1} for water vapor molecules on PAMPS than 50 wt.% TiO_2 NWs/PAMPS composite material films coated on QCM. This demonstrated that water vapor molecules were easier to be dissociated from the PAMPS films. Moreover, molecular mechanics calculation supported the results that the larger sensitivity of 50 wt.% TiO_2 NWs/PAMPS composite material films to water vapor molecules might to be ascribed to the slightly larger association constant K than PAMPS films.

Acknowledgements

The authors thank the National Science Council (grant nos. NSC 93-2216-E-235-001 and NSC 94-2216-E-034-007) of Taiwan for support.

References

[1] P.R. Story, D.W. Galipeau, R.D. Mileham, Sens. Actuators B 24–25 (1995) 681.

[2] C. Cantalini, M. Pelino, J. Am. Ceram. Soc. 75 (1992) 546–551.

[3] H. Yagi, M. Nakata, J. Ceram. Soc. Jpn. 100 (1992) 152.

[4] W.P. Tai, J.H. Oh, Sens. Actuators B 85 (2002) 154.

[5] Q. Wan, Q.H. Li, Y.J. Chen, T.H. Wang, X.L. He, X.G. Gao, J.P. Li, Appl. Phys. Lett. 84 (2004) 3085.

[6] J.P. Randin, F. Züllig, Sens. Actuators 11 (1987) 319.

[7] Y. Sakai, V.L. Sadaoka, M. Matsuguchi, Polym. Bull. 18 (1987) 501.

[8] J.P. Gong, N. Komatsu, T. Nitta, Y. Osada, J. Phys. Chem. B 101 (1997) 740.

[9] Y. Sakai, M. Matsuguchi, N. Yonesato, Electrochim. Acta 46 (2001) 1509.

[10] P.G. Su, I.C. Chen, R.J. Wu, Anal. Chim. Acta 449 (2001) 103.

[11] C.D. Feng, S.L. Sun, H. Wang, C.U. Segre, J.R. Stetter, Sens. Actuators B 40 (1997) 217.

[12] J. Wang, B. Xu, J. Zhang, G. Liu, T. Zhang, F. Qiu, M. Zhao, J. Mater. Sci. Lett. 18 (1999) 1603.

[13] J. Wang, Q. Lin, T. Zhang, R. Zhou, B. Xu, Sens. Actuators B 81 (2002) 248.

[14] J. Wang, B.K. Xu, S.P. Ruan, S.P. Wang, Mater. Chem. Phys. 78 (2003) 746.

[15] Y. Sakai, Y. Sadaoka, M. Matsuguchi, Sens. Actuators B 35–36 (1996) 85.

[16] P.R. Somani, A.K. Viswanath, R.C. Aiyer, S. Radhakrishnan, Sens. Actuators B 80 (2001) 141.

[17] S.P. Lee, K.J. Park, Sens. Actuators B 35–36 (1996) 80.

[18] A. Star, T.-R. Han, V. Joshi, J.R. Stetter, Electroanalysis 16 (2004) 108.

[19] M. Penza, G. Cassano, Sens. Actuators B 68 (2000) 300.

[20] M. Neshkova, R. Petrova, V. Petrov, Anal. Chim. Acta 332 (1996) 93.

[21] F.P. Delannoy, B. Sorli, A. Boyer, Sens. Actuators A 84 (2000) 285.

[22] L.X. Sun, T. Okada, Anal. Chim. Acta 421 (2000) 83.

[23] S. Mintova, T. Bein, Microporous Mesoporous Mater. 50 (2001) 159.

[24] H.W. Chen, R.J. Wu, K.H. Chan, Y.L. Sun, P.G. Su, Sens. Actuators B 104 (2005) 80.

[25] A.J. Cunningham, Introduction to Bioanalytical Sensors, Wiley, New York, 1998, p. 307.

[26] G. Sauerbrey, Z. Phys. 155 (1959) 206.

[27] Y.X. Zhang, G.H. Li, Y.X. Jin, Y. Zhang, J. Zhang, L.D. Zhang, Chem. Phys. Lett. 365 (2002) 300–304.

[28] M.B. Kulwicki, J. Am. Ceram. Soc. 74 (1991) 697.

[29] R. Schaub, P. Thostrup, N. Lopez, E. Laegsgaard, I. Stensgaard, J.K. Norskov, F. Besenbacher, Phys. Rev. Lett. 87 (2001) 266104.

[30] Y. Okahata, M. Kawase, K. Niikura, F. Ohtake, H. Furusawa, Y. Ebara, Anal. Chem. 70 (1998) 1288–1296.